doi.org/10.1002/cbdv.202300030 Research Article CHEMISTRY & BIODIVERSITY

www.cb.wiley.com

Copper(II) Complexes Derived from Schiff Bases Containing 4-Methylbenzylamine as a Core Unit: Cytotoxicity, pBR322-DNA Studies, Biological Assays, and Quantum Chemical Parameters

Dasari Shiva Shankar,[a, c] Aveli Rambabu,[b] Swathi M,[a] P. V. Anantha Lakshmi,[a] and Shivaraj*[a]

Bivalent copper complexes, $[Cu(SB^1)_2]$ **1** (SB^1 = (2-(4-methylbenzylimino)methyl)-5-methylphenol, $[Cu(SB^2)_2]$ **2** (SB^2 = (2-(4-methylbenzylimino)methyl)-4-bromolphenol), and $[Cu(SB^3)_2]$ **3** (SB^3 = (2-(4-methylbenzylimino)methyl)-4,6-dibromophenol) were synthesized using the Schiff bases prepared from 4-methylbenzylamine (*p*-tolylmethanamine). These were characterized using a variety of spectro-analytical methods. For all copper complexes, a square planar geometry was determined through spectral analyses. Utilizing molecular orbital energies, the stability of the copper complexes was calculated from quantum chemical characteristics. The kinetic and thermal degradation parameters were calculated from the thermograms. Studies on DNA binding interactions, such as UV absorption and emission, have shown that the manner of DNA binding is intercalative, and the binding constant (K_b) order is **3** > **2** > **1**. Under oxidative and photolytic techniques, the copper complexes outperform the parent Schiff bases in their ability to cleave double-stranded pBR322 DNA. When tested for cytotoxicity on the KB3 and MCF7 cell lines, complexes displayed greater activity than their parent ligands. Studies on the complexes' in-vitro antibacterial and antioxidant activity showed that they are significantly more powerful than the parent ligands.

Introduction

There has been a plethora of research that focus on the evolution of new metal-based compounds with high biological potency against DNA. There are several studies on Schiff base complexes due to their widespread biological activities in the past few decades, such as antioxidant, antidiabetic, anticancer, antimicrobial, anti-inflammatory.[1] Still as there is a scope, the chemists and biochemists focused on creating transition metal complexes that act as chemical nucleases for plasmid nicking or direct strand scission. The chemistry of copper, among transition metals, is predominantly aimed at occupying the cisplatin position.[2] Copper components often do not mediate nucleobase oxidation; instead, they are in charge of direct strand scission through hydrogen atom removal from the deoxyribose section. Since it is important for many enzymes and has a distinct mechanism of action than cisplatin and other platinum medicines, copper complexes are considered as the best alternative for cisplatin.[3]

The interaction of DNA with Cu(II) complexes has been shown to exhibit a wide spectrum of biological characteristics in vitro.[4,5] Today, numerous investigations on copper complexes of ligands containing phenyl groups have demonstrated that ligands strengthen the binding contact of complexes with DNA by improving the planarity of the molecule.[6–8] Furthermore, the copper complexes having the ligands that are rich with N, O and S like atoms increase the biological potency.[9–12] The ligands containing phenyl groups as core units have manifold biological applications including bacterial, fungicide, antioxidant and anticancer agents.[13–16] The Schiff bases' aromatic moiety is crucial in enhancing DNA binding affinity.[17] Due to their great biocompatibility and low toxicity (LD50 [median fatal dose] 1670 mg kg^{-1} for males and 1900 mg kg^{-1} for females]), Schiff bases with copper complexes have received a lot of attention in the biosciences.[18,19]

The pre-emptive theoretical studies are convenient to predict the biological efficacy of newly synthesized drugs of transition metals. Keeping the above findings in mind, our research group focused on the transition metal complexes of diverse biologically active Schiff bases containing benzothiazole, isoxazole and furfurylamine as core units.[20–23] As an extension of our group research, in this investigation, we focused on the design and preparation of copper based metal complexes from the Schiff bases derived from 4-methyl benzylamine, given in Scheme 1. Our precise work demonstrated that the molecular orbital (HOMO & LUMO) energies, thermal and kinetic parameters, DNA interaction and biological activities.

[a] *D. S. Shankar, S. M, P. V. A. Lakshmi, Shivaraj*
Department of Chemistry, Osmania University, Hyderabad – 500007, Telangana, India
E-mail: srajkavadi@gmail.com

[b] *A. Rambabu*
Department of Science and Humanities, St. Martin's Engineering College, Dhulapally, Hyderabad – 500100, Telangana, India

[c] *D. S. Shankar*
Deartment of Chemistry, Post Graduate College, Osmania University, 502249 Mirzapur

Supporting information for this article is available on the WWW under https://doi.org/10.1002/cbdv.202300030

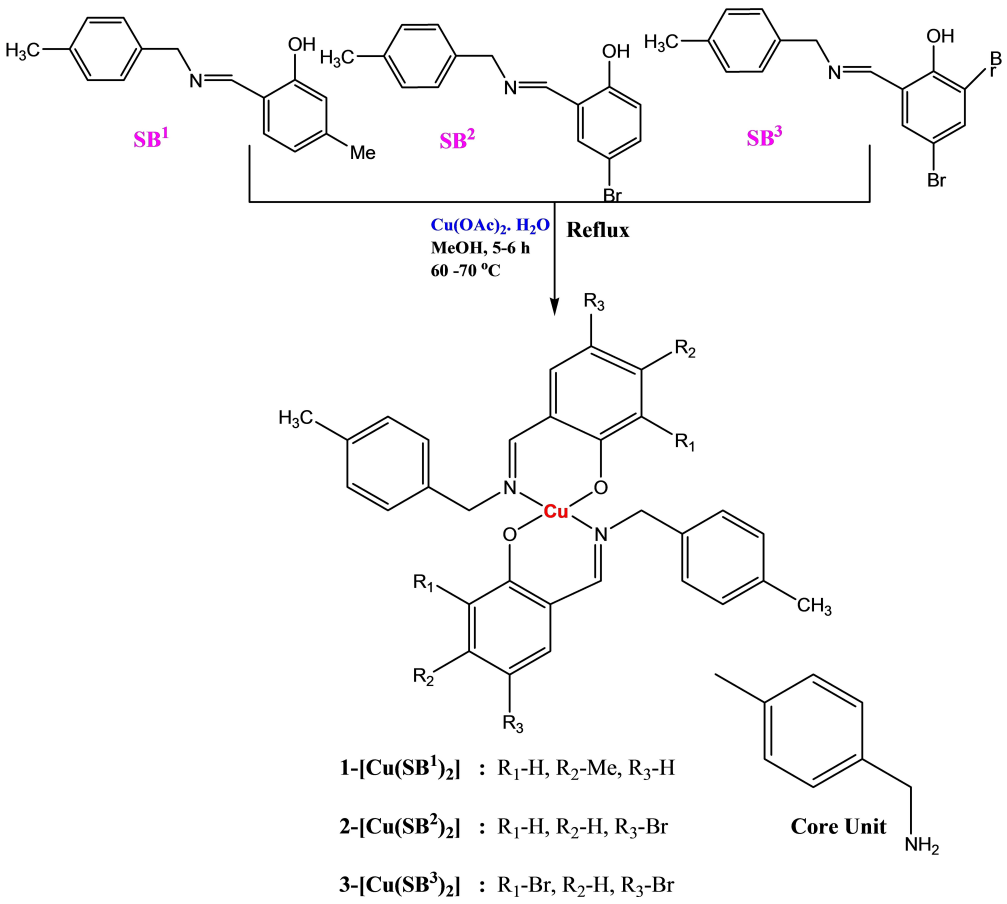

Scheme 1. The synthetic route for Copper(II) complexes (**1**–**3**).

Result and Discussion

Characterization of ligands and copper complexes

The colored 4-methylbenzylamine (*p*-tolylmethanamine) Schiff bases (SB^{1-3}) were synthesized in a conventional method. They were highly stable at room temperature and non-hygroscopic. The analytical data obtained for all complexes are in good agreement with 1:2 stoichiometric ratios of metal to ligand (*Supporting Information* (SI)).

From the FT-IR spectra of complexes, the broad band that the free ligands exhibited between 3442 and 3445 cm^{-1} is vanished in complexes, indicating that the phenolic –OH group participated in coordination with the metal ion by losing its proton. It is possible that the mode of coordination occurred through the azomethine nitrogen atoms with the metal centers because the azomethine (–CH=N–) stretching that caused by the strong ligands in the region of 1623–1637 cm^{-1} is shifted in complexes towards lower/higher wave number by the difference of 1–14 cm^{-1}.[24] Due to M–O and M–N stretching vibrations, two non-ligand bands are come into sight in the lower frequency region, 595–614 cm^{-1} and 425–479 cm^{-1}, respectively.[25] The corresponding data and images are depicted in SI (Table 1), and Figure S1 (SI), respectively. The UV/VIS absorption spectral images of the synthesized ligands and their complexes are shown in Figure S2 (SI), and the data is presented in SI (Table 2). Due to the $^2B_{1g}$-^2E_g d-d transition in the visible region, copper complexes (**1**–**3**) displayed a broad band at 575 to 622 nm, which is compatible with a square planar geometry,[26] and ESI-MASS (*m/z*) of metal complexes shown in SI.

Table 1. EPR parameters.

Complex	$g_{\parallel}$	$g\perp$	g_{ave}	$A_{\parallel}$	α^2	β^2	γ^2	$K^2{}_{\parallel}$	$K^2\perp$	G	μ_{eff}
1	2.157	2.053	2.087	0.0189	0.652	1.109	1.454	0.724	0.237	3.051	1.808
2	2.136	2.057	2.080	0.0204	0.622	1.027	1.681	0.639	0.261	2.066	1.804
3	2.073	2.037	2.062	0.0191	0.589	0.573	1.125	0.337	0.165	2.017	1.774

Table 2. Thermal decomposition data.

Complex	Molecular formula	Steps	Temp. °C	Weight loss (%) Found	Calc.	Assignment
1	$CuC_{32}H_{32}N_2O_2$	1	30-300°C	50.64	50.79	$C_{16}H_{18}N_2$
		2	300-570°C	41.15	41.24	$C_{16}H_{14}O_2$
2	$CuC_{30}H_{26}Br_2N_2O_2$	3	>570°C(residue)	08.21	08.76	CuO (residue)
		1	32.4-200°C	49.62	49.83	$C_{16}H_{12}Br_2$
3	$CuC_{30}H_{24}Br_4N_2O_2$	2	200-535°C	38.36	38.67	$C_{14}H_{14}N_2O_2$
		3	>535°C (residue)	12.02	12.27	CuO (residue)
		1	31.3-300°C	51.31	51.69	$C_{14}H_{16}Br_2NO$
		2	300-615°C	38.43	38.72	$C_{16}H_8Br_2NO$
		3	>615°C (residue)	10.26	10.45	CuO (residue)

EPR spectra

The hyperfine and super hyperfine structures of copper complexes can be examined using EPR spectroscopy which is extremely helpful in analyzing the metal ion environment in complexes. Spectral images are shown in Figure 1 and the parameters $g_{\|}$, $g_{\perp}$, g_{av} and G values that were determined and presented in Table 3. The hyperfine coupling constants for complexes **1**–**3** were found to be between 0.0189 and 0.0204 cm^{-1}.

The exchange coupling contacts between the two copper centers are measured by the anisotropic parameter "G" which can be calculated by the Kneubuhi method.[27] Where $G=(g_{\|}-2.0023)/(g_{\perp}-2.0023)$, and the 'G' values are found to be 2.017 to 3.051, which are less than 4 showing that exchange interactions are significant.[28] The following equations were used to determine the molecular orbital coefficients of α^2 (covalent in-plane bonding), β^2 (covalent in-plane bonding), and γ^2 (out-plane bonding),[29]

$$\alpha^2 = (A\| / 0.036) + (g\| - 2.0023) + (3/7)(g\perp - 2.0023) + 0.04 \quad (1)$$

$$\beta^2 = \frac{(g\| - 2.0023)\,E}{-8\,\lambda\alpha^2} \quad (2)$$

$$\gamma^2 = \frac{(g\perp - 2.0023)\,E}{-2\,\lambda\alpha^2} \quad (3)$$

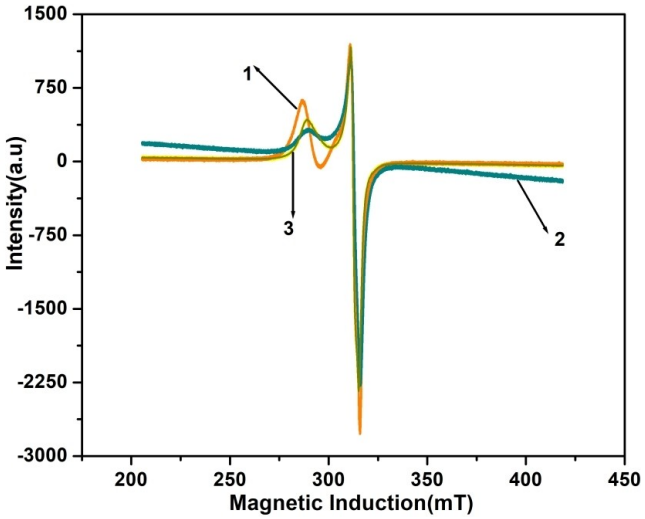

Figure 1. EPR spectra of Copper (II) complexes (**1**–**3**).

Where, *E* is the electronic transition energy, and $\lambda = -828$ which represents the free copper ion. As we known, α^2 value of 0.5 indicates a complete covalent bond, while a value of 1.0 denotes a pure ionic bond. According to Table 1, the values of α^2 (0.589 to 0.652) clearly demonstrated that the in-plane σ-bonding has a strong covalent character compared to in-plane π-bonding β^2 (0.573 to 1.109) and out-plane π-bonding γ^2 is (1.125 to 1.681). These findings are in agreement with previous reported values,[30] [a]nd the following formulas are used to compute the bonding parameters;

$$K^2_{\|} = \frac{[(g_{\|} - 2.0023)\,\Delta E]}{8\lambda^o} \quad (4)$$

Table 3. Kinetic parameters.

Complex	Stage	E ($J\,mole^{-1}$)	A (S^{-1})	△S ($J\,mole^{-1}K^{-1}$)	△H ($J\,mole^{-1}$)	△G	R
1	I	4.29×10^6	1.43×10^5	-0.14×10^2	4.10×10^6	7.40×10^6	0.976
2	I	8.16×10^6	6.38×10^5	-0.13×10^3	7.91×10^6	1.19×10^6	0.980
3	I	1.06×10^7	2.74×10^8	-0.08×10^2	1.03×10^6	1.31×10^6	0.995

$$K^2_{\perp} = \frac{[(g_{\parallel} - 2.0023)\,\Delta E]}{2\lambda^o} \quad (5)$$

Hathaway expressed that for pure σ-bonding, $K^2_{\parallel} = K^2\perp = 0.77$; for in-plane π-bonding, $K^2_{\parallel} < K^2_{\perp}$, and for out-plane π-bonding $K^2_{\parallel} > K^2_{\perp}$. Here, $K^2_{\parallel} > K^2_{\perp}$; which shows that out-plane bonding is present. Additionally, the following equation is used to determine the magnetic moment (μ_{eff}) from the ESR measurements;

$$\mu_{eff} = \frac{1}{2}(g_{||}{}^2 + 2\,g_{\perp}{}^2)^{1/2} \quad (6)$$

Thermogravimetric analysis

A useful method to assess the compounds' thermal stability and mass loss% is thermogravimetric analysis (TGA). Thermograms of this study are displayed in Figure 2, and the decomposition stages of the beginning and end temperature, and weight loss assignments are shown in Table 2. In the current study, the weight loss of complexes **1**–**3** was measured in the temperature range of 10 to 1000 °C, with the metal complexes heating rates being adequately controlled at 10 °C min^{-1} in a N_2 atmosphere. According to the data, complexes thermally decompose primarily in two phases. The remarkable thermal stability of complexes **2** and **3** up to 200 °C affirms that there is no solvent or water molecule inside or outside the coordination sphere. In the first stage, all the complexes (**1**–**3**) displayed a sudden weight loss between 295 and 350 °C. The steady weight loss that occurs in the temperature range above 390 °C during the secondary decomposition step may be interpreted as the complete decomposition of the organic material around the metal ion, and the remaining horizontal line may represent CuO residue.

Thermal decomposition kinetics

According to the Coats-Redfern (CR) equation, the plot will be linear with a significant correlation coefficient if the proper model is used for the response. The kinetic and thermodynamic parameters of the thermal degradation of TM-HBO complexes derived from the model with the best linear fit are presented in Table 3. Several CR models for complexes **1**–**3** in terms of *ln[g(α) / T²] vs. 1/T* are shown in Figure S6, with correlation coefficient ranges from 0.976 to 0.995, all models suggest a linear trend.

HOMO-LUMO studies

The compounds were created using the Perkin Elmer ChemBio Draw software, and their bond lengths, bond angles, and torsional angles were optimized using the Perkin Elmer ChemBio3D ultraprogram. The optimized values are reported in SI (Table 4). Quantum chemical parameters are derived using the energies of HOMO (highest occupied molecular orbital) and LUMO (lowest unoccupied molecular orbital) structures; the stability of the complexes (**1**–**3**) was examined in Figure 3.

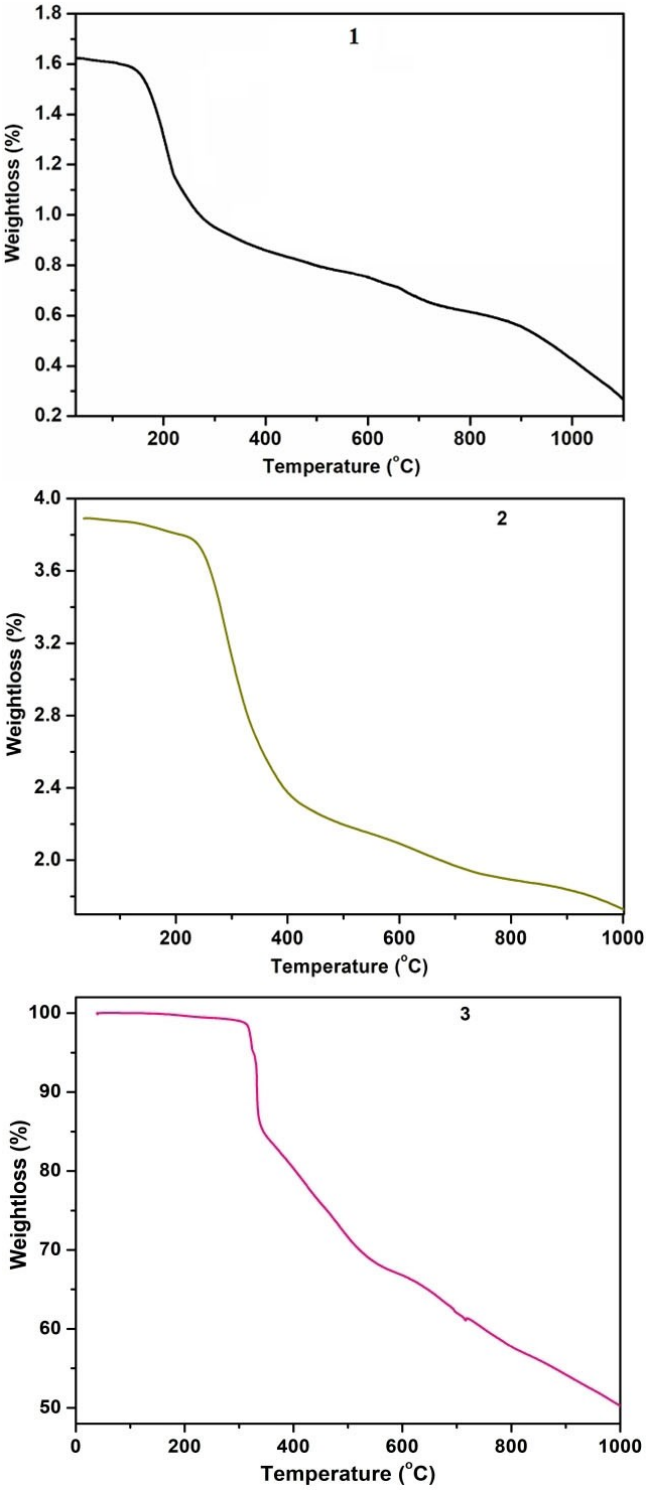

Figure 2. Thermograms of Copper complexes (**1**–**3**).

Table 4. Quantum chemical parameters.

Compound	HOMO	LUMO	E_g(eV)	χ (eV)	η (eV)	σ (eV)	P_i (eV)	S (eV)	ω (eV)	$\triangle N_{max}$
SB[1]	−9.986	−2.281	7.705	6.1335	3.852	0.259	−6.133	0.129	4.882	1.592
SB[2]	−9.963	−2.505	7.458	6.234	3.729	0.268	−6.234	0.134	5.210	1.671
SB[3]	−9.923	−2.353	7.570	6.138	3.785	0.264	−6.138	0.132	4.976	1.621
1	−7.052	−2.505	4.547	4.7785	2.273	0.439	−4.778	0.219	5.021	2.101
2	−7.123	−2.739	4.384	4.931	2.192	0.456	−4.931	0.228	5.546	2.249
3	−7.117	−2.573	4.544	4.845	2.272	0.440	−4.845	0.220	5.165	2.132

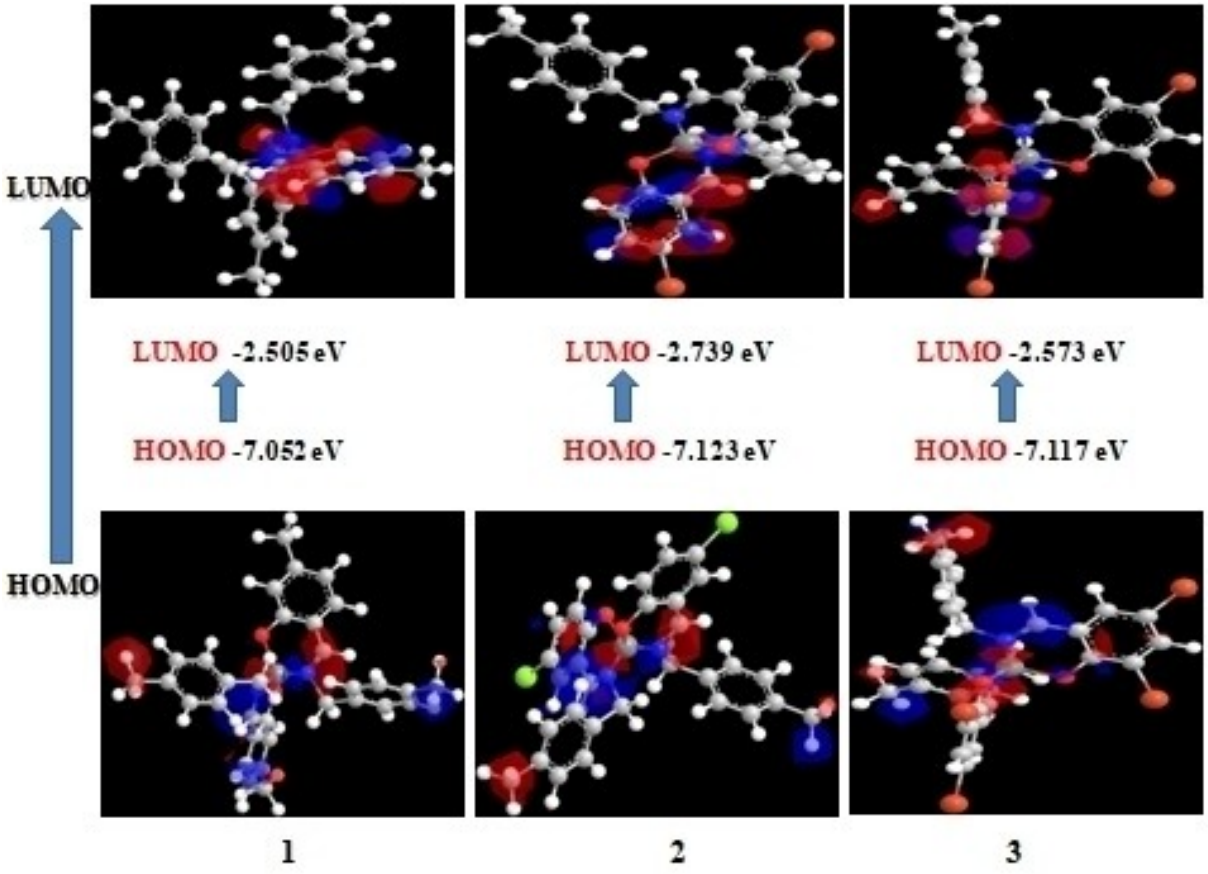

Figure 3. Molecular orbital structures of complexes (**1**–**3**).

HOMO stands for the ability to donate an electron, and LUMO for the ability to accept an electron. The molecules' *ionization energy* and *electron affinity* calculations were done using their molecular orbital energies. Calculations are used to determine quantum chemical properties of complexes, such as the energies of the HOMO and LUMO. The energy gap (E_g) values of complexes are in the range of 4.384 to 4.547 eV. A small energy gap denotes a complex' higher reactivity,[31] in that way the complex **2** had the highest reactivity. Further parameters, like the molecular orbitals energy gap E_g, absolute electro negativity, chemical potential, π, absolute hardness, η, absolute softness, σ, global electrophilicity, ω, global softness, S, and additional electronic charge N_{max}, calculated using equations[32] (listed in SI) are formulated in Table 4.

DNA binding studies

To find out the binding modes and capacity of metal complexes towards DNA is to monitor how the absorbance spectra change when they are introduced to increasing amounts of DNA. The strength of the intercalation interaction is commensurate with the degree of the hypochromism and red shift.[33] The complexes situate themselves in the center of the DNA double helix and are inserted between two stacked base pairs of DNA. The complexes are sustained by hydrophobic stacking interactions with the neighboring base pairs when they are intercalated to the DNA base pairs, which lowers the π–π* transition energy and causes bathochromism. The three complexes' binding constant (K_b) values are found to be, $1.81 \pm 0.34 \times 10^4$ (**1**), $2.97 \pm 0.51 \times 10^4$ (**2**) and $4.83 \pm 0.35 \times 10^5$ (**3**), respectively. The stretched planar aromatic moiety and halogen

(bromo) substituted groups in complexes **2** and **3** may be the cause of their enhanced binding affinity.[34,35] Due to the presence of two bromo groups, complex **3** appeared to have a larger affinity for DNA than the other two complexes (**3** > **2** > **1**). Figure 4 exhibits the complexes from a perspective.

The emission spectra of EB-DNA were examined in the current investigation both in the presence and absence of quencher metal complexes (0–60 μM). Due to the displacement of EB bound-DNA by complexes, the emission intensity of the EB is reduced upon the addition of complexes (Figure 5). The complexes were capable of attaching to DNA through the intercalation mode. $3.21 \pm 0.45 \times 10^4\ M^{-1}$ (**3**), $2.59 \pm 0.23 \times 10^4\ M^{-1}$ (**2**), and $2.36 \pm 0.01 \times 10^4\ M^{-1}$ (**1**) are the computed quenching constant (K_{SV}) values.

Nuclease efficacy

The characteristic oxidative and photolytic cleavage ability of complexes (**1**-**3**) against supercoiled (SC) pBR322 DNA was ascertained using the *gel electrophoresis* method. Figure 6(**a**) and (**b**) show the results of cleavage capacity of three complexes, which demonstrate that **a** and **b** did not display any significant cleavage in Lane-1 (DNA control). However, Lanes 6 to 8 in oxidative cleavage and Lanes 5 to 7 (**1**–**3**) in the photolytic method displayed a good cleavage pattern, particularly in the presence of H_2O_2, where the DNA was effectively cleaved up to Form-III. Lanes 3 to 5 in oxidative cleavage and Lanes 2 to 4 (ligands) in photolytic method showed a little cleavage.

Molecular oxygen or diffusible hydroxyl radicals, both of which are capable of damaging DNA by Haber-Weiss type chemistry,[36,37] when copper ions interact with H_2O_2 in an oxidative cleavage process, leading to the cleavage of SC pBR322 DNA. DNA cleavage occurs as a result of $^1O_2$ critical role in the photolytic cleavage pathway. According to Toshima et al., the triplet states produced by the π–π* and n–π* photo excitation in the UV irradiation are the main causes for the formation of $^1O_2$ from activated oxygen.

Cytotoxicity

Cytotoxicity is hypothesized by the influence of affinity of complexes towards DNA. We employed the MTT assay to compare the cytotoxicity of prepared complexes **1**–**3** to that of the widely prescribed anticancer drug, cisplatin. For this study, oral cancer cell lines, KB3 and human breast cell lines, MCF-7 were examined. Cell viability was estimated in terms of percentage. A dose-dependent increase in cell mortality was observed after each of the drugs was applied to the KB3and MCF-7 cell lines. The complexes were more cytotoxic than the free ligands due to the presence of the metallic centers. As shown in Table 5 and graphs, ligands and their complexes (**1**–**3**) showed different anticancer activity against a wide range of cell lines when compared to cisplatin.

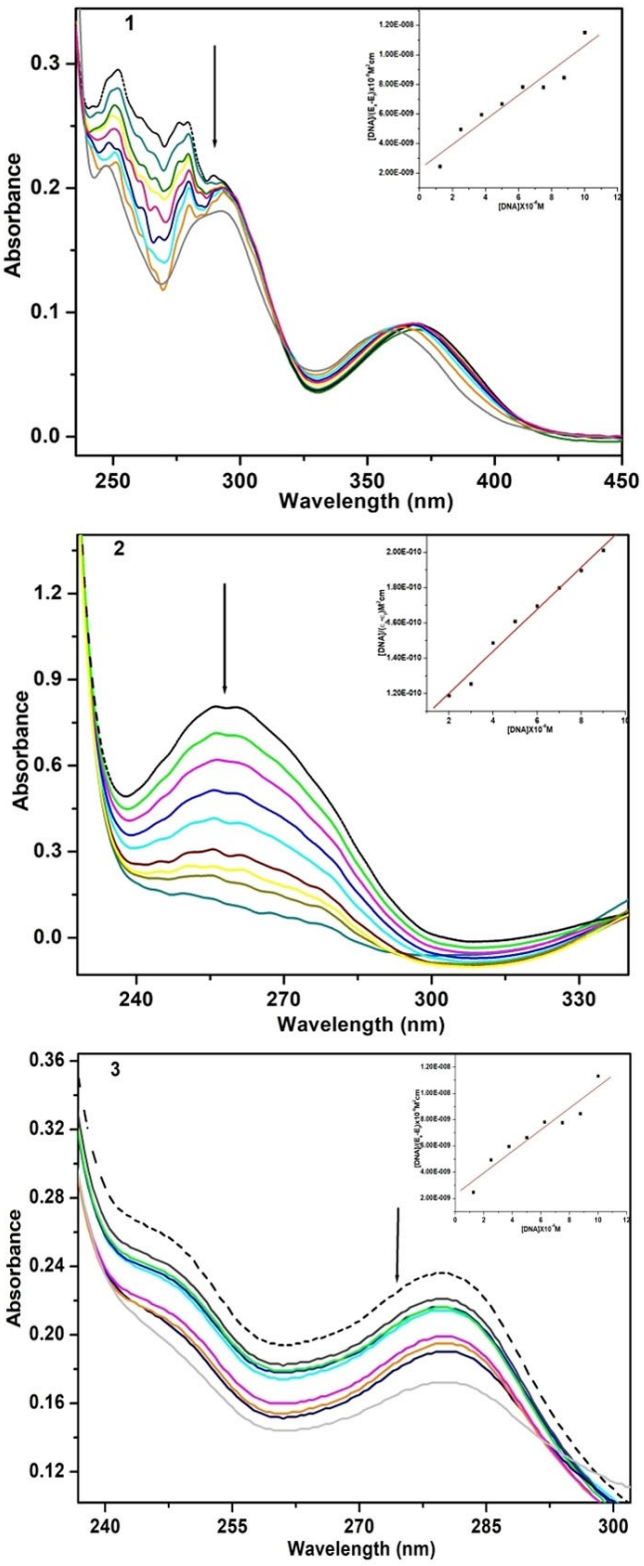

Figure 4. Absence (dotted line) and presence (solid lines) of increasing CT-DNA concentrations in Tris-HCl buffer in the absorption spectra of Copper complexes (**1**–**3**) (pH 7.2). Conditions: [DNA] = 0–10 μM, [Complex] = 10 μM, Inset: linear plot.

On cocytes that had been subjected to the test compounds / complexes showed alterations in morphology. It is noticeable

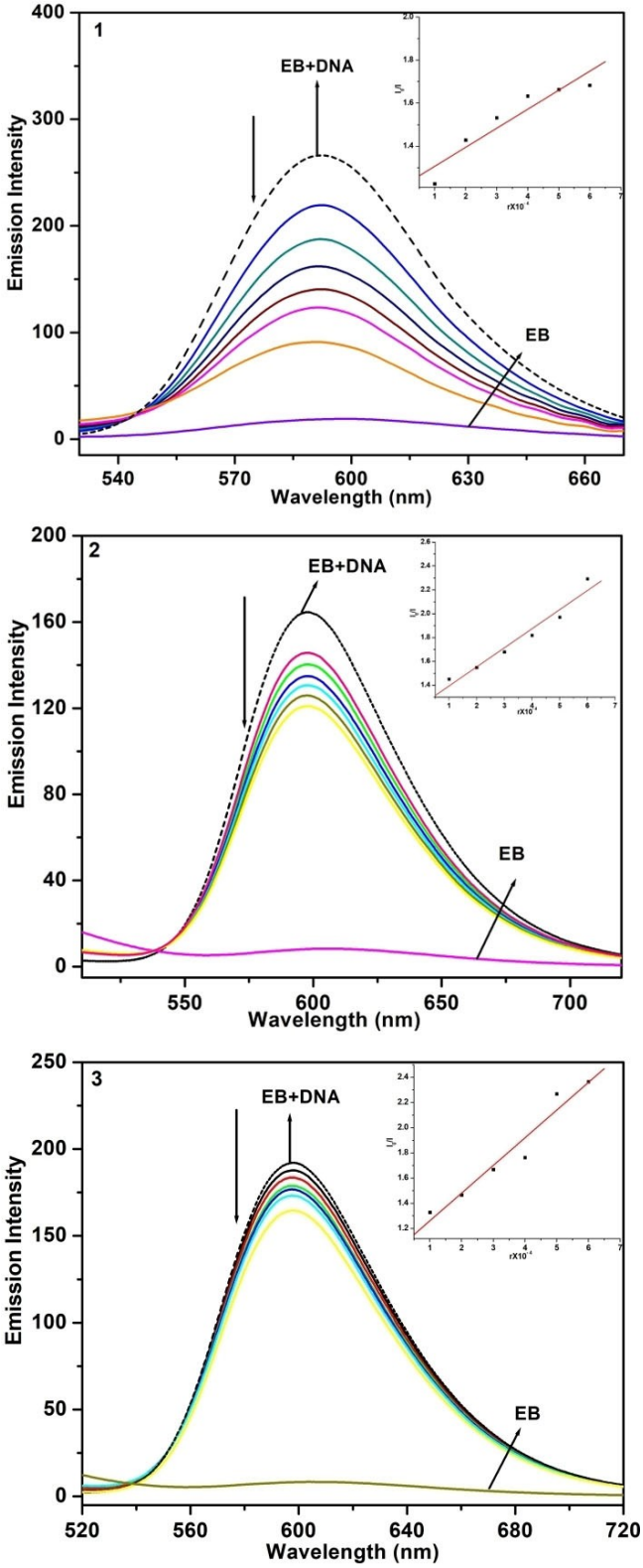

Figure 5. Emission intensity of EB bound-DNA (12.5 μM) in the absence and presence (different concentrations) of complexes (**1**–**3**), where [DNA]-=125 μM, Tris-HCl + 50 μM NaCl buffer, pH = 7, and [Complex] = 0 - 60 μM, respectively.

Table 5. IC_{50} values (μM) of the test compounds.

Compound	IC_{50} values (μM) MCF7	KB3
SB^1	27 ± 0.21	25 ± 0.51
SB^2	24 ± 0.41	24 ± 0.21
SB^3	21 ± 0.1	18 ± 0.65
1	14 ± 0.58	16 ± 0.91
2	12 ± 0.31	09 ± 0.45
3	8.2 ± 0.5	7.5 ± 0.42
Cisplatin	< 2.27	< 2.52

that combining Schiff bases with copper complexes has a significant impact on cytotoxicity because the inhibitory activity of complexes was significantly higher than that of their respective ligands. Apart from complexes **1** and **2**, the complex **3** has greater anticancer activity against both cell lines, as evidenced by lower IC_{50} values, which may be attributed to the di-bromo functional groups (electron-withdrawing). The cytotoxicity (Figure 7) of complexes is in well consistent with the binding affinity values.

DPPH radical scavenging

One of the popular and simple colorimetric ways to assess the radical-scavenging capacity of synthesized compounds is the DPPH method. The scavenging action increases in a dose-dependent manner as the complex concentration rises. Ascorbic acid (AA) is employed as a positive control, as shown in Figure 8. The IC_{50} values were calculated and presented in Table 6. Complex **3** (08.56 ± 0.63) showed a highest radical scavenging activity than other two copper complexes and lesser than the standard drug (AA), and the order is given as Vitamin C > **3** > **2** > **1**. The complexes **1** and **2** have moderate radical scavenging activity with 13.63 ± 1.76 and 11.74 ± 1.45.

Antibacterial assay

With respect to the two bacterial strains *B. thuringiensis* (gram + ve), and *E. coli* (gram -ve), the three complexes (**1**-**3**) exhibit noticeable antibacterial activity at four different doses. The zone of inhibition values of ligands as well as complexes were given in Table 7 and illustrated as Figure 9. It is evident that the Cu(II) complexes' zone of inhibition is slightly larger than that of free Schiff bases. Both the Overtone hypothesis and Tweedy's chelation theory can account for the complexes' increased antibacterial potency.[38, 39]

Table 6. IC_{50} values of synthesized copper complexes.

Compound	IC_{50} (μM)
AA	0.42 ± 2.03
1	13.63 ± 1.76
2	11.74 ± 1.45
3	07.56 ± 0.63

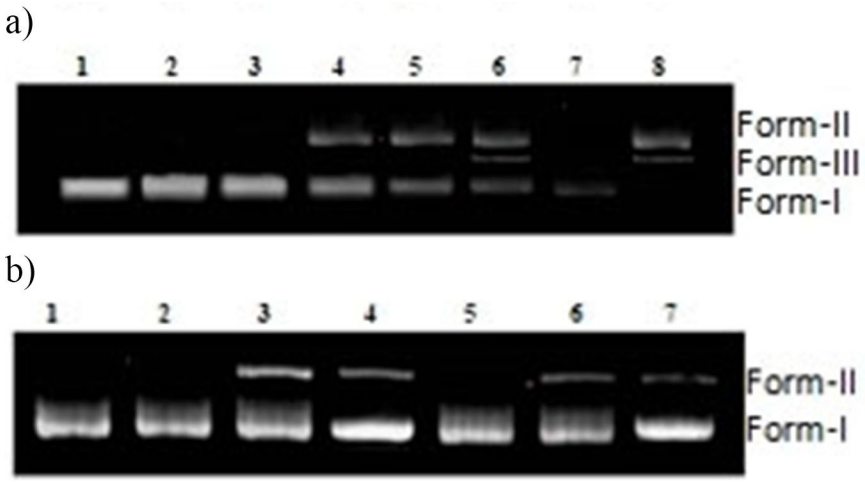

Figure 6. (**a**). Oxidative cleavage ability of ligands and their Cu(II) complexes, **1–3** against SC pBR322-DNA (0.2 g, 33.3 μM) at 37 °C in 5 μM Tris-HCl/5 μM NaCl buffer. Lane 1: DNA control; Lane 2: DNA + H_2O_2 (2 μM); Lane 3: DNA + H_2O_2 (2 μM) + SB^1; Lane 4: DNA + H_2O_2 (2 μM) + SB^2; Lane 5: DNA + H_2O_2 (2 μM) + SB^3; Lane 6: DNA + H_2O_2 (2 μM) + 1; Lane 7: DNA + H_2O_2 (2 μM) plus 2; and Lane 8, DNA + H_2O_2 (2 mM) + **3** (2 μM). (**b**). Photolytic cleavage ability of ligands and their Cu(II) complexes, **1–3** against SC pBR322-DNA using 365 nm UV light at 37 °C, and 5 μM Tris-HCl/5 μM NaCl buffer. Lane 1, DNA control; Lane 2, DNA + SB^1 (4 μM); Lane 3, DNA + SB^2 (4 μM); Lane 4, DNA + SB^3 (4 μM); Lane 5, DNA + complex **1** (4 μM); Lane 6, DNA + complex **2** (4 μM); Lane 7, DNA + complex **3** (4 μM).

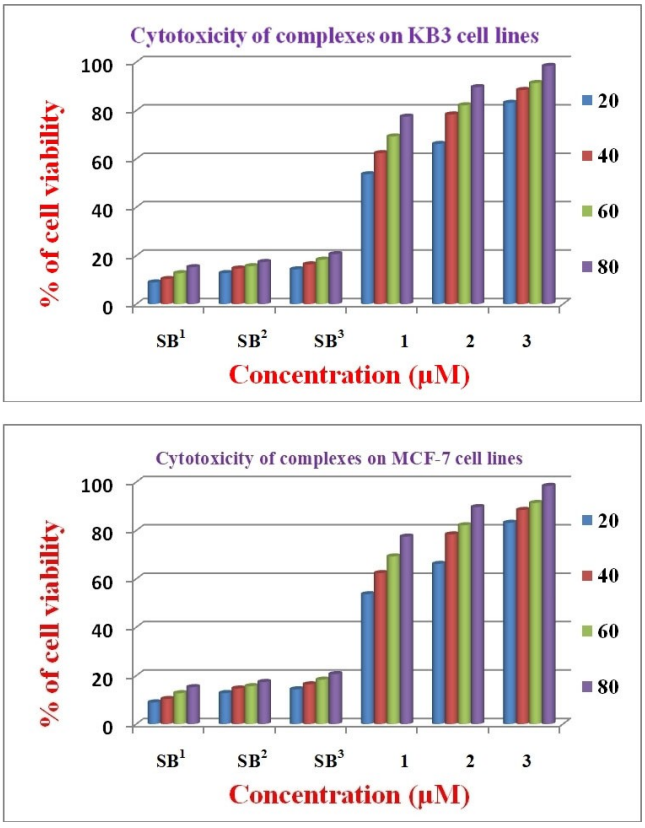

Figure 7. Cytotoxicity of test compounds on KB3 and MCF7 cell lines.

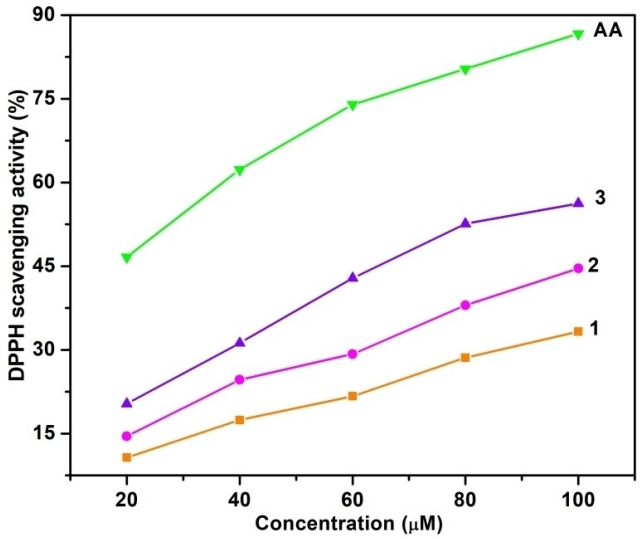

Figure 8. Scavenging activity of Cu(II) complexes on DPPH radicals.

According to Overtone's theory of cell permeability, the lipid membrane that encircles the cell prefers the passage of only the lipid-soluble components, making liposolubility a significant factor that governs the activity of bacteria. Chelation, on the other hand, greatly reduces the polarity of the metal ion due to the partial sharing of its positive charge with the donor groups as well as due to the delocalization of the π-electron on the entire chelating ring. This, in turn, increases the lipophilic nature of the central metal atom, which favour its permeation more effectively through the lipid layer of cell membrane, thereby more aggressively destroying them.

Conclusions

The three prepared copper complexes, **1–3** own a square planar geometry, evidenced by different spectro-analytical methods. The complexes undergo non-spontaneous thermal breakdown, but kinetic studies reveal that they are thermally stable. All the

Table 7. Zone of inhibition data.

Compound	Zone of inhibition (mm) Gram +ve *B. thuringiensis* 25 μg/mL	50 μg/mL	75 μg/mL	100 μg/mL	Gram −ve *E. coli* 25 μg/mL	50 μg/mL	75 μg/mL	100 μg/mL
SB^1	1.03 ± 0.3	1.07 ± 0.1	1.11 ± 0.2	1.16 ± 0.3	1.04 ± 0.2	1.09 ± 0.2	1.13 ± 0.1	1.15 ± 0.2
SB^2	1.04 ± 0.1	1.03 ± 0.2	1.05 ± 0.3	1.07 ± 0.1	1.05 ± 0.2	1.07 ± 0.3	1.11 ± 0.3	1.16 ± 0.4
SB^3	1.06 ± 0.2	1.05 + 0.1	1.06 ± 0.1	1.12 ± 0.2	1.05 ± 0.3	1.07 ± 0.2	1.12 ± 0.2	1.18 ± 0.5
1	1.33 ± 0.1	1.35 ± 0.3	1.36 ± 0.2	1.39 ± 0.1	1.34 ± 0.1	1.39 + 0.1	1.42 ± 0.4	1.49 ± 0.2
2	1.35 ± 0.2	1.39 ± 0.2	1.42 ± 0.3	1.46 ± 0.2	1.36 ± 0.3	1.42 ± 0.3	1.46 ± 0.2	1.56 ± 0.3
3	1.46 ± 0.4	1.49 ± 0.3	1.56 ± 0.4	1.63 ± 0.1	1.53 ± 0.1	1.59 ± 0.4	1.63 ± 0.3	1.79 ± 0.1
Ampicillin	2.1 ± 0.4	2.1 ± 0.2	2.1 ± 0.4	2.1 ± 0.3	2.2 ± 0.3	2.2 ± 0.2	2.2 ± 0.1	2.2 ± 0.2

Standard deviation (±).

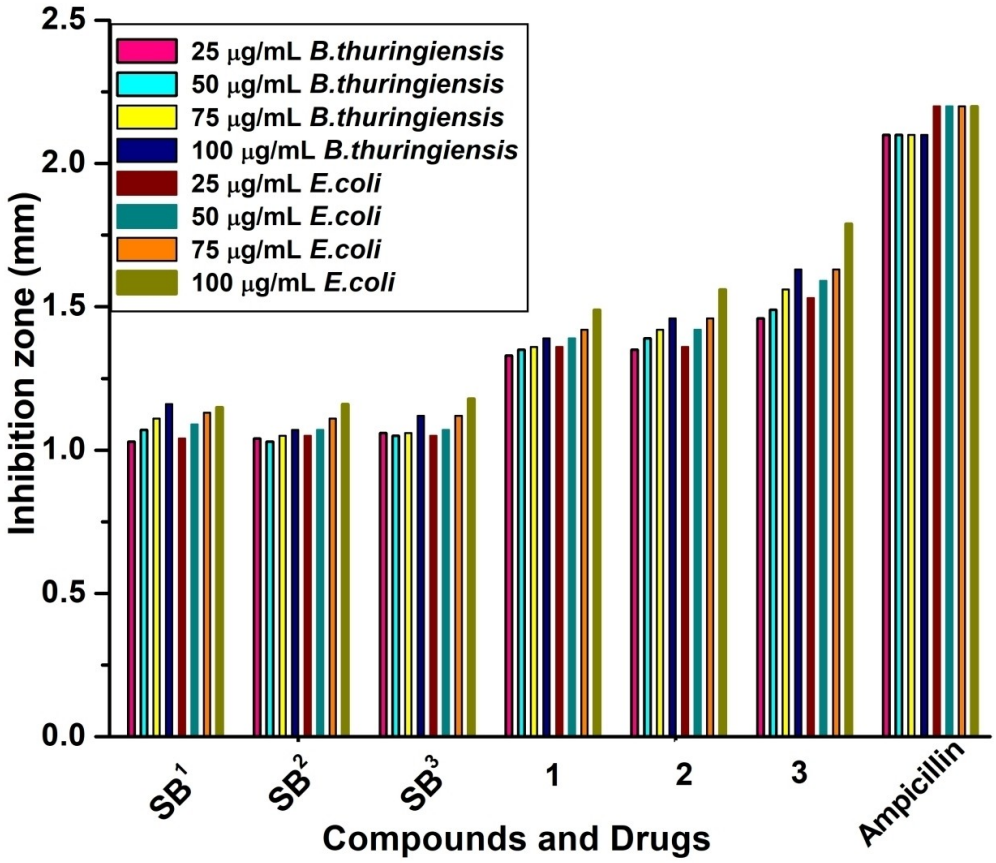

Figure 9. Antibacterial activity graph of ligands and their complexes tested against bacterial strains.

kinetic parameters determined by Coats-Redfern method proved that the Cu(II) complexes show good results. The stability of the complexes increases with an increase in the aromaticity of the ligands when they bind to the CT-DNA via an intercalation mechanism of binding. Additionally, these complexes exhibited DNA incision propensities of the order of **3** > **2** > **1**. The cell viability test confirmed that the complex **3** has demonstrates strong anticancer potency against KB3 and MCF-7 cell lines compared to other compounds. Complex **3** showed stronger radical scavenging activity than the other two but less than the standard. The complexes are more efficacious than free ligands, according to studies done on two bacterial strains. This will helpful in future to find out the insights of metal complexes produced based on Schiff bases containing heterocyclic moieties.

Author Contributions

Dasari Shiva Shankar: Data curation; formal analysis; investigation; validation; visualization. Aveli Rambabu: Data curation; review & editing; validation. Swathi M: Data curation. P.V. Anantha Lakshmi: Data curation; investigation; resources; soft-

ware. Shivaraj: Conceptualization; methodology; resources; validation; supervision.

Acknowledgements

We thank the Chemistry Department Head for giving the tools necessary to complete the assignment successfully. We acknowledge the spectral and analytical data that were provided by the Director CFRD at Osmania University, the Director IICT in Hyderabad, and the SAIF at IIT Bombay. We are grateful and also thankful to DST-SERB (SB/EMEQ-141/2014) for providing financial support to department of chemistry. We thank UGC-BSR faculty fellowship scheme for providing financial support. One of the authors (Prof. Shivaraj) thank UGC New Delhi for awarding BSR faculty fellowship (No.26-13/2020 (BSR)); 27.09.2021.

Conflict of Interests

The authors declare no conflict of interest.

Data Availability Statement

The data that support the findings of this study are available in the supplementary material of this article.

Keywords: copper complex · cytotoxicity · DNA interaction · biological activity · quantum chemical parameters

[1] H. Zhu, Y. Hu, C. Li, X. W. Wang, X. Y. Yang, *Chem. Rev.* **2014**, *114*, 5572–5610.
[2] P. Kumar, S. Gorai, M. K. Santra, B. Mondal, D. Manna, *Dalton Trans.* **2012**, *41*, 7581.
[3] C. J. Burrows, J. G. Muller, *Chem. Rev.* **1998**, *98*, 1109.
[4] N. H. Williams, B. Takasaki, M. Wall, J. Chin, *Acc. Chem. Res.* **1999**, *32*, 493.
[5] G. Y. Li, K. J. Du, J. Q. Wang, J. W. Liang, J. F. Kou, X. J. Hou, L. N. Ji, H. Chao, *J. Inorg. Biochem.* **2012**. *119*, 53.
[6] J. Leng, Z. Shang, Y. Quan, *Inorg. Chem. Commun.* **2018**, *91*, 123.
[7] A. Rambabu, N. Ganji, S. Daravath, K. Venkateswarlu, K. Rangan, Shivaraj, *J. Mol. Struct.* **2020**, *1199*, 127006.
[8] F. M. Alkhatib, T. A. Farghaly, M. F. Harras, H. A. El-Ghamry, *Inorg Nano-Met Chem.* **2021**, https://doi.org/10.1080/24701556.2021.2011319.
[9] H. A. El-Ghamry, M. Gaber, T. A. Farghaly, *Mini Rev. Med. Chem.* **2019**, *19*, 1079.
[10] S. Zehra, M. S. Khan, I. Ahmad, F. Arjmand, *J. Biomol. Struct. Dyn.* **2019**, *37*, 1879.
[11] S. Kathiresan, S. Mugesh, J. Annaraj, M. Murugan, *New J. Chem.* **2017**, *41*, 1283.
[12] T. Vijayan, A. Jayamani, S. Nallathambi, *Eur. J. Med. Chem.* **2015**, *89*, 278.
[13] A. Rambabu, M. P. Kumar, N. Ganji, S. Daravath, Shivaraj, *J. Biomol. Struct. Dyn.* **2020**, *38*, 316.
[14] B. S. Demir, S. Ince, M. K. Yilmaz, A. S. E. Derinoz, T. Taskin-Tok, Yasemin Saygideger, *Pharmaceutics.* **2022**, *14*, 2409.
[15] P. Kumar, B. Narasimhan, K. Ramasamy, V. Mani, R. K. Mishra, R. K. Majeed, *Curr. Top. Med. Chem.* **2015**, *15*, 1050–1066.
[16] N. Ganji, A. Rambabu, N. Vamsikrishna, S. Daravath, Shivaraj, *J. Mol. Struct.* **2018**, *1175*, 173–182.
[17] L. H. Abdel-Rahman, R. M. El-Khatib, L. A. E. Nassr, A. M. Abu-Dief, M. Ismail, A. A. Seleem, *Spectrochim. Acta* **2014**, *117*, 366–378.
[18] P. Kavitha, M. R. Chary, B. V. V. A. Singavarapu, K. L. Reddy, *J. Saudi. Chem. Soc.* **2016**, *20*, 80.
[19] P. Kumar, S. Gorai, M. K. Santra, B. MondaL, D. Manna, *Dalton Trans.* **2012**, *41*, 7573–7581.
[20] S. Tejaswi, M. P. Kumar, A. Rambabu, N. Vamsikrishna, Shivaraj, *J Fluoresc.* https://doi.org/10.1007/s10895-016-1911-3.
[21] M. P. Kumar, N. Vamsikrishna, G. Ramesh, N. J. P. Subhashini, N. J. Babu, Shivaraj, *J. Coord. Chem.* **2017**, *70*, 1388.
[22] G. Nirmala, V. K. Chityala, M. P. Kumar, A. Rambabu, N. Vamsikrishna, D. Sreenu, Shivaraj, *J. Photochem. Photobiol. B Biol.* **2017**, *175*, 140.
[23] K. Venkateswarlu, M. P. Kumar, A. Rambabu, N. Vamsikrishna, D. Sreenu, K. Rangan, Shivaraj, *J. Mol. Struct.* **2018**, *1160*, 207.
[24] A. Kanwal, B. Parveen, R. Ashraf, N. Haider, K. G. Ali, *J. Coordination Chem.* **2022**, https://doi.org/10.1080/00958972.2022.2138364.
[25] V. Rajendiran, R. Karthik, M. Palaniandavar, H. Stoeckli-Evans, V. Subbarayan Periasamy, M. Abdulkader Akbarsha, B. Suresh Srinag, H. Krishnamurthy, *Inorg. Chem.* **2007**, *46*, 8208–8221.
[26] V. P. Singh, *Spectrochim. Acta Part A.* **2008**, *71*, 22.
[27] K. Venkateswarlu, A. Rambabu, D. S. Shankar, P. V. A. Lakshmi, Shivaraj, *Chem Biodiversity.* **2022**, *19*, e202100686.
[28] P. Bindu, M. R. P. Kurup, T. R. Satyakeerty, *Polyhedron.* **1999**, *18*, 321.
[29] N. Vamsikrishna, M. P. Kumar, G. Ramesh, N. Ganji, S. Daravath, Shivraj, *J. Chem. Sci.* **2017**, *129*, 622.
[30] K. Venkateswarlu, P. V. Anantha Lakshmi, Shivaraj, *Appl Organomet Chem.* **2022**, *36*, e6530. https://doi.org/10.1002/aoc.6530.
[31] B. Shekhar, P. Vasantha, B. S. Kumar, P. V. Anantha Lakshmi, *Appl Organometal Chem.* **2018**, e4254, https://doi.org/10.1002/aoc.4254.
[32] K. Rajeshwari1, P. Vasantha, B. S. Kumar, P. V. Anantha Lakshmi, *Biol. Trace Elem. Res.* https://doi.org/10.1007/s12011-022-03100-1.
[33] S. Daravath, A. Rambabu, N. Ganji, G. Ramesh, P. V. Anantha Lakshmi, Shivaraj, *J. Mol. Struct.* **2022**, *1249*, 131601.
[34] R. Loganathan, M. Ganeshpandian, N. S. P. Bhuvanesh, M. Palaniandavar, A. Murugananthan, S. K. Ghosh, A. Riyasdeen, M. A. Akbarsha, *J. Inorg. Biochem.* **2017**, *174*, 13.
[35] B. Barut, U. Demirbas, A. Ozel, H. Kantekin, *Int. J. Biol. Macromol.* **2017**, *105*, 499.
[36] A. M. El-badrawy, A. A. Fadda, E. Abdel-Latif, Y. A. Selim, *RSC Advances.* **2021**, *11*, 34308.
[37] A. T. Gordona, O. O. Abosedea, S. Ntsimangob, S. Vuurenc, E. C. Hostena, A. S. Ogunlaja, *Inorg. Chim. Acta.* **2020**, *510*, 119744.
[38] D. H. Cai, C. L. Zhang, Q. Y. Liu, L. He, Y. J. Liu, Y. H. Xiong, X. YiLe, *Eur. J. Med. Chem.* **2021**, *213*, 113182. https://doi.org/10.1016/j.ejmech.2021.113182.
[39] L. Liu, Z. Yao, S. Wang, T. Xie, G. Wu, H. Zhang, P. Zhang, Y. Wu, H. Yuan, H. Sun, *J. Med. Chem.* **2021**, *64*, 8391–8409.

Manuscript received: January 6, 2023
Accepted manuscript online: May 31, 2023
Version of record online: ■■, ■■■